JOURNAL OF MATERIALS SCIENCE **38** (2003) 1367–1375

Review
Stability of nanostructured materials

R. A. ANDRIEVSKI
Institute of Problems of Chemical Physics, Russian Academy of Sciences, Chernogolovka, Moscow Region, 142432, Russia
E-mail: ara@icp.ac.ru

The different aspects of nanostructured material (NM) stability such as thermal and chemical stability as well as NM behavior under deformation and radiation are characterized and analyzed in detail. Grain growth, phase transitions (including spinodal decomposition), homogenization diffusion processes, relaxation of residual stresses, and behavior of grain boundary and triple junction segregations are discussed in context of the change of nanostructure and properties. Special interest is given to the availability of NMs with ultra-fine grain size and their behavior during annealing as soon as to the possibility of development of nanostructures with high thermal stability. Some unsolved problems are emphasized.

1. Introduction

It is well known that almost all NMs except supramolecular structures are usually far from equilibrium state [1, 2]. Many features such as a large share of interfaces and triple junctions, possible irregular distribution of alloying elements and admixtures, the occurrence of non-equilibrium phases and supersaturated solutions, residual stresses, and excess concentrations of lattice defects increase the Gibbs free energy. All these features are closely connected with non-equilibrium conditions of the NM preparation such as powder technology methods, controlled crystallization from molten state, severe plastic deformation, and film/coating technology (Table I) [2].

It follows from general considerations that the thermal activation and other effects such as radiation, deformation and chemical reactions lead to the enhancement of diffusion, relaxation and recrystallization with partial or total annihilation of the nanocrystalline structure, non-equilibrium phases and residual stresses that are responsible for the NM properties. There are many important characteristics of structural and functional NMs which are strongly depended from thermal and other stability. This is especially important for cutting materials and for high-temperature friction applications; thermal and diffusion barriers; high-temperature catalysts and semiconductors; porous, emission and filter components; structures with giant magnetoresistance and so on. Therefore an understanding of factors that affect NM stability and degradation is critical to identifying the best strategies for future technology development.

Some recent papers and books (e.g. [1–10] were devoted for the most part to the grain growth in NMs. The present review is an attempt to give a consideration of the NM stability as a whole taking in account all aspect regarding metals, alloys, intermetallics, oxides, borides, nitrides, etc., both in nanostructured bulk and film form.

2. Thermal stability

2.1. General considerations

Grain growth, relaxation of residual stresses, phase transitions (including deomposition of non-equilibrium phases and supersaturated solid solutions), and segregation/homogenisation diffusion processes arise from thermal effect. All these phenomena are familiar in general materials science but in the case of NMs the nanoscale peculiarities make their examination and understanding not so easy. In addition, many different methods of preparation (Table I) and many structural types of NMs (according to opinion [1] there are 12 types of nanostructure in NMs) complicate the interpretation and comparison. It is also necessary to point that some obtained results reflect not only the behavior of consolidated bulks and films but that for individual particles produced by mechanical alloying, sliding wear and so on. All things considered, the present author tries to point some general features and connect them with preparation methods. Some aspects of NM thermal stability have analysed by present author earlier [11].

2.2. Grain growth

2.2.1. Experimental data

Figs 1–7 show some experimental results on the temperature and duration effects on grain growth and hardness in different NMs. From these data and other suitable information, the following considerations are noteworthy.

1. Numerous studies of kinetics have revealed a lot of diverse information. It was shown that in many cases the grain growth mechanism can not be based on the

TABLE I Main methods of consolidated NM preparation

Group	Variation	Object
Powder technology	Gleiter's method (vapour-phase deposition) and compacting; conventional pressing and sintering; rate-controlled sintering; electric-discharge sintering; hot working (hot pressing, forging, extrusion, etc.); high static and dynamic pressure at room and high temperatures	Elements, alloys, compounds
Severe plastic deformation	High pressure torsion Equal channel angular pressing Rolling/extrusion of manylayer composites Transformation-induced hardening	Deformable metals and alloys
Controlled crystallization from amorphous state	Conventional and high pressures	Amorphous materials
Film/coating technology	PVD and CVD Electrodeposition Sol-gel methods	Elements, alloys, compounds

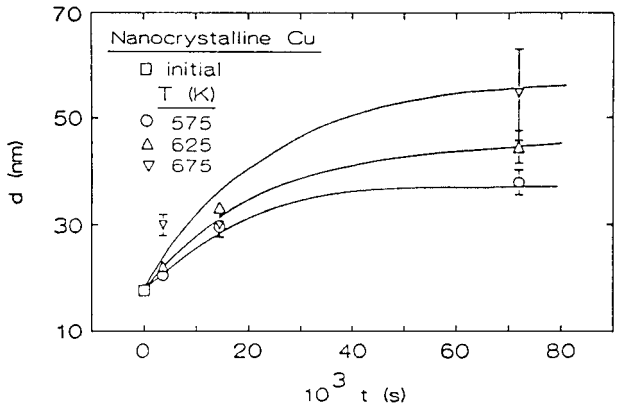

Figure 1 Kinetics of grain growth of nano-Cu obtained by sliding wear [12].

unique value of exponent n (i.e., as $L \sim t^n$ where L is the grain size and t is time) because the data revealed fit for several values of n (1/2, 1/3 or 1/4) (Fig. 1) [12]. The annealing of the $NbAl_3$ nanocrystals obtained by mechanical alloying [13] and $Fe_{33}Zr_{67}$ or $(Fe, Co)_{33}Zr_{67}$ alloys obtained by crystallisation from an amorphous state [14] tended to the relationship of $L \sim t^{1/3}$. The detail investigation of annealing of nano-RuAl prepared by mechanical alloying has shown that isothermal grain growth fits the following relationship

$$\frac{L^2(t) - L^2_{\max}}{L^2(0) - L^2_{\max}} = \exp\left[-\frac{2qt}{L^2_{\max}}\right] \quad (1)$$

where q is the rate constant; $L(t)$, $L(0)$ and $L_{\max}$ are the grain size at annealing time t, initial grain size and maximum that respectively (Fig. 2) [15].

2. The exponent n can depend not only on subjects but on temperature interval also $(1/n = 0.05–0.5)$ [1, 7]. The deviation from ideal value of 0.5 (this value is deduced from known parabolic relationship for grain growth in coarse-grained materials) is connected with many factors such as pores and impurity doping, temperature change of the grain growth mechanism, initial grain size distribution and so on. Therefore, the activation energy (Q) values for isothermal grain growth have also a wide dispersion. For example the Q values for nanocrystalline Fe prepared by mechanical attrition

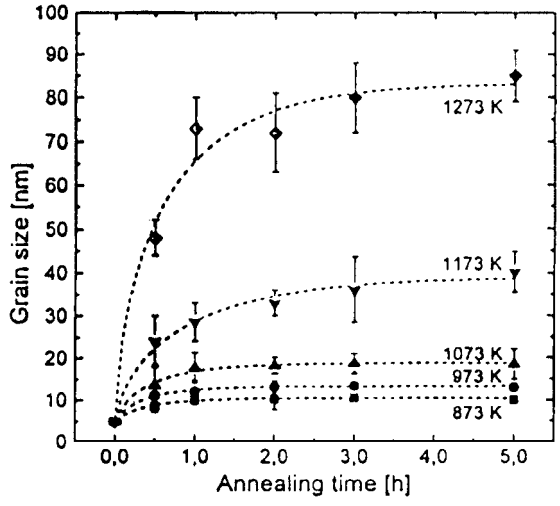

Figure 2 Grain size of nano-RuAl as a function of annealing at different temperatures. Points indicates measured data and dashed lines are fitted with Equation 1 [15].

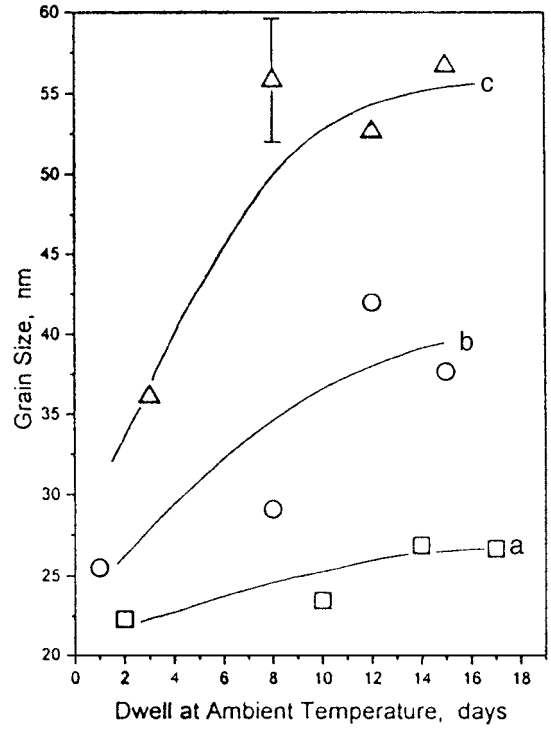

Figure 3 The time-dependence of grain size at ambient temperature for nanocrystalline copper specimens obtained by evaporation—condensation with following consolidation (Gleiter's method) and differed by relative bulk density: a–93%; b–96%; c–97% [17].

in two intervals of annealing temperature ($T < 500$°C and $T > 500$°C) were found to be of 125 kJ/mol and 248 kJ/mol respectively [5]. Both values are lower than corresponding ones for grain boundary diffusion (∼175 kJ/mol) and the lattice diffusion (∼270 kJ/mol) in Fe.

3. Some results show that the grain growth in several specimens of Cu (Fig. 3), Ag, and Pd [16, 17] as soon as of nitride multilayers [4] can be observed under long duration at room and near temperatures. The effect of pores as Zener drags on the inhibition of grain growth is also evident (Fig. 3).

4. The log-normal or normal distributions of grain size are typical for many NMs in initial and annealed state. However, abnormal grain growth has been observed in some cases including long-temperature endurance [17]. Such behavior can be considered as a possible result of non-uniformity of the initial grain size distribution in the as-prepared specimens or/and of non-uniform admixture segregation [1, 17].

5. Cryomilling of Fe-Al powders leads to a significant increase of thermal stability as compared with pure nanocrystalline Fe (Fig. 4) [18]. This situation may be to connected with a pinning by fine particles of $FeAl_2O_4$ and a solute segregation mechanism. Some interstitial impurities such as oxygen and nitrogen result also at the oxide and nitride formation, and that is why the start of grain growth shifts to the high-temperature interval in the case of Ag-O, Ti-N and Mo-N systems [16, 19]. The grain boundary pinning by oxide and nitride phases seem to be likely present.

6. The superior thermal stability of the duplex microstructure has been observed for the Cu-Ag, Ag-MgO and TiN-Si_3N_4 nanocomposites both in the bulk and film form [16, 20, 21].

7. The recrystallization features at heat treatment up to 1000°–1100°C have been studied for individual, alloyed and multilayer films of TiN, ZrN, NbN, and CrN [4, 22–24]. The dependences of hardness on thickness (h), layers (bilayer period $\lambda = 100$) and alloying for ZrN films are demonstrated on Fig. 5 [23]. It is evident that the decrease of h to a value of 0.1 μm is accompanied by the recrystallization start lowering to about 200 K. The

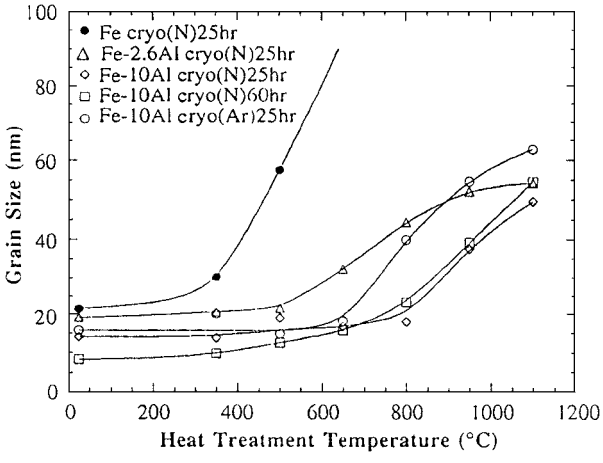

Figure 4 Grain size of cryomilled powders Fe-Al after 1 h heat treatment. Legend indicates powder composition in weight percent, cryogenic media in parentheses, and milling time [18].

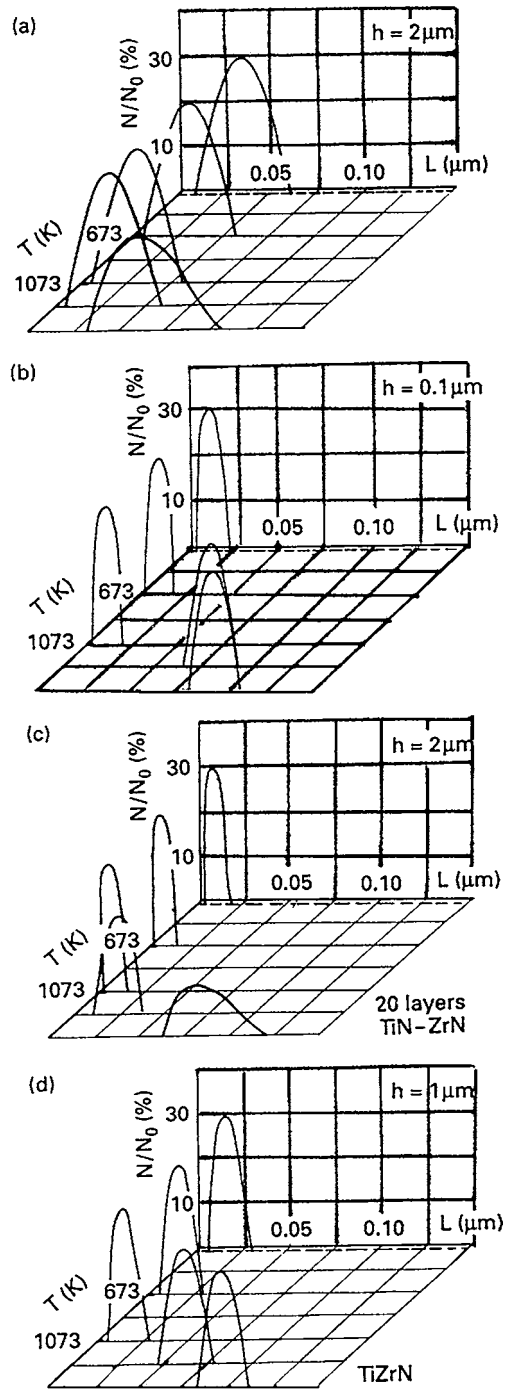

Figure 5 Statistical distribution curves for ZrN films: (a) h $= 2$ μm; (b) $h = 0.1$ μm; (c) ZrN/TiN, 20 layers; (d) alloyed film ($Zr_{0.5}$ $Ti_{0.5}$)N [23]. Duration of vacuum annealing was of 20 min.

recrystallization start in multilayer films is nearly the same as for individual films with a thickness of about 0.1 μm. However, the recrystallization rate in the multilayer case can be lower because of a possible effect of residual compressive stresses and interphase boundaries. The comparison of the recrystallization rates for the individual and alloyed and films revealed that grain growth in the latter is lower. The behaviour of other type films (TiN, AlN, NbN, and CrN) is essentially the same. Very interesting result has been revealed in the case of TiN/AlN multilayer films with very low λ [24]. As is clear from Fig. 6, the thermal stability of multilayer with λ of 2.9 nm was reported to be higher then that for sample with $\lambda = 16$ nm.

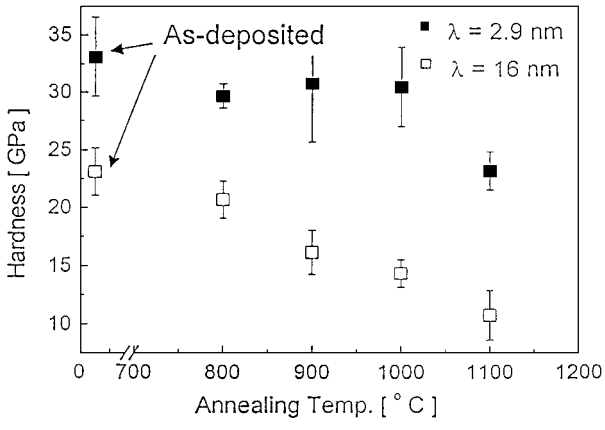

Figure 6 Hardness of TiN/AlN multilayers with different bilayer period (λ) as a function of annealing temperature in Ar atmosphere ($t = 2$ hr; the whole thickness of films was about 300 nm) [24].

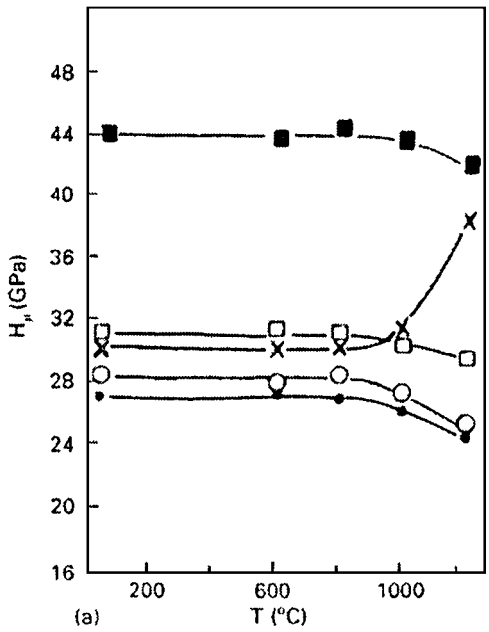

Figure 7 Hardness films (thickness of 2 μm) as a function of annealing temperature [22]. Key: ■ TiN/ZrN ($\lambda = 100$); □ TiN/ZrN ($\lambda = 200$); × (Ti,Zr)N; ● ZrN; ○ TiN.

8. An annealing of NMs is accompanied by the change of many physical-mechanical properties such as strength, hardness (see Figs 6 and 7), electrical and elastic characteristics and so on. However, the changes are determined not only by grain growth but also by other structure parameters such as microstrains, residual stresses, relaxation of elastic strain, spinodal decomposition (see in Fig. 7 data for (Ti,Zr)N films), ordering, etc. The numerous similar examples of the property thermal stability of metallic NMs prepared by severe plastic deformation can be found in book [9]. It is well known that the defects initiated by deformation are not so thermal stable and annihilate mainly before recrystallization. A relatively high thermal stability has been observed for the $Cu + 0.5\%Al_2O_3$ nanoalloy processed by internal oxidation and severe plastic torsion [25].

2.2.2. Some theoretical approximations

It follows from general considerations that grain growth can be stopped by the grain boundary mobility control and due to an action of a thermodynamic driving force.

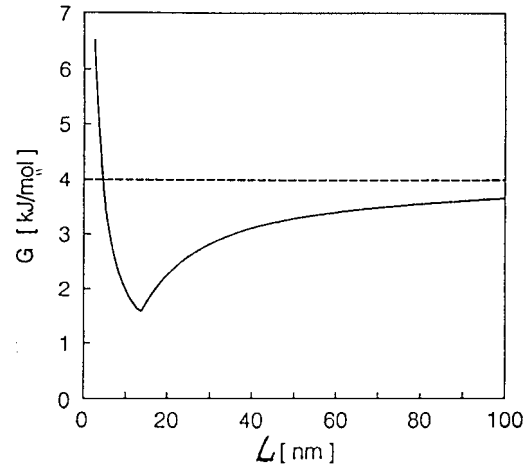

Figure 8 Variation of the molar Gibbs free energy G of a binary alloy polycrystal with grain size L at fixed P, T, and fixed overall solute concentration $x_\beta = 0.05$. The dotted line denotes the Gibbs free energy og the solid solution single crystal with the same x_β [28].

Aside from the well known considerations on effect of Zener drag, pinning of grain boundaries by pores, solute atoms or inclusions, and decrease of grain boundary energy [1, 2, 7, 26, 27], it seems to be necessary to call attention to some other points. For example, the alloy effects in nanostructures have been analysed in [28–30] and it was shown that a minimum on the total molar Gibbs free energy for some alloys can exist in the nanocrystalline region (Fig. 8). This result has been obtained in both the Langmuir-McLean approximation [28] and in the Fowler-Guggenheim one [30]. The availability of this minimum implies a possibility to inhibit the grain growth process and stabilise the nanocrystalline structure if the initial grain size values are lower than those which correspond to of the Gibbs free energy minimum. In addition to the above-stated information on nano-RuAl (Fig. 2) [15, 27], there are also some other examples of the grain growth prevention in nanocrystalline alloys Y-Fe [31], Pd-Zr [29], and Ni-P [1, 32]. The grain growth decrease in these cases is considered to be connected with the segregation effect.

Another possibility of thermodynamic stabilisation of grain growth in NMs has been pointed out in [33]. Taking into account that grain growth is accompanied by the 'injection' of vacancies into the bulk of material and thus by of the Gibbs free energy increase, it is possible to estimate the critical grain size L_C below which 'locking' of grain growth occurs

$$L_C/2 = \left[24NkTZ(\delta\beta d)^2 \frac{m}{D_{SD}}\right]^{1/3} \qquad (2)$$

Where δ, β and m are the grain boundary characteristics: thickness, the relative excess free volume and mobility; N is the Avogadro number; Z is coordination number; kT has usual manner; D_{SD} is the bulk self-diffusion coefficient, and d is characteristic vacancy sink spacing. For $L_O < L_C$ the generated vacancy supersaturation inhibits grain growth but at $L_O > L_C$ grain growth can be realised by common way following for example to the parabolic law ($\sim t^2$).

It should be noted that the vacancy generation during the grain boundary growth has been observed in

the positron-annihilation study of recrystallization of ultrafine powder [34] and confirmed by a molecular dynamics simulation [35].

If the dislocation availability in NMs is unlikely and the vacancy sinks are provided by grain boundaries ($L_C/2 \sim d$) the relationship (2) changes to

$$L_C/2 = 24NkTZ(\delta\beta)^2 \frac{m}{D_{SD}} \quad (3)$$

Taking for Al the values $m = 2 \times 10^{-14}$ m^4 J^{-1} S^{-1} ($T = 300$°C) and $D_{SD} = 1.3 \times 10^{-17}$ m^2/s one obtains $L_C/2$ of the order 100 nm that is typical maximum grain size in NMs [33].

Using of the relationships (2) or (3) it is profitable to take in mind the estimation of the characteristic length of the lattice-dislocation stability Λ

$$\Lambda = \alpha Gb/2\tau_p \quad (4)$$

where α is the coefficient of the dislocation geometry of 0.1–10, G is the shear modulus, b is the Burgers vector, and τ_p is the Peierls stress [36]. In the case of $L < \Lambda$ the lattice dislocations tend to leave the crystals. The Λ values (in nm) for edge dislocations in some metals [36] and titanium nitride [37] are the following

Cu	Al	Ni	Fe	TiN
25	10	10	2	∼1

When $L_C < \Lambda$ it is a good reason to use the relationship (3) but in the situation of $L_C > \Lambda$ the Equation 2 is better to apply. However, in both cases it is necessary to remember the approximate nature of the relationships (1–4).

One more feature of the NM nanostructure lies in a great number of triple junctions. The inhibition of the triple junction effect on grain growth has been demonstrated in [8, 38, 39]. Molecular dynamics simulation also suggested that the triple junction drag is important at the small grain size, low temperature and high symmetry grain misorientations [40]. The main conclusion is that the triple junction effect must always be considered in the case of the NM thermal stability.

Thus the theoretical considerations as regarding to the inhibition of grain growth by the grain boundary mobility control [8, 38–40] and the thermodynamic driven force (e.g. [28, 33]) suggest that there is possibility to create the thermally stabile NMs with very fine grain size. Some experimental evidence relating to films of TiN/AlN (Fig. 6) [24], Cu and Au [41] as well as to nanocrystalline alloy $Ni_{80}P_{20}$ [42]) confirm this statement. A phenomenological description of the grain growth stagnation for nanocrystalline films and powders has been discussed in [43]. However, many details of these approaches (i.e., the more precise definition of optimal grain size, comparison of different methods for the grain growth inhibition and so on) need further accurate study.

2.3. Phase transitions

The non-equilibrium processing of NMs results not only in nanocrystalline structure but also in the presence of the non-equilibrium phases and supersaturated solid solutions. These metastable structures are especially an inherent feature of NMs prepared by mechanical alloying and film/coating technology. The formation of supersaturated solid solutions and non-equilibrium phases has been observed in the systems of Fe-Cu, Fe-Ni, Fe-Ti, Fe-A1, W-Cu, Ni-Al, TiN-TiB_2, TiN-AlN, and so on (e.g. [4, 18, 37, 44–51]). The significant increase of the component mutual solubility has been revealed. The polymorphic phase stability in thin multilayers of Co/Cr and Al/Ti has been analysed in [52]. Unfortunately, the thermal stability data of these subjects is not so comprehensive. There is some information for the Fe-Cu, Fe-Ni, and TiN-TiB_2 systems [44, 46, 47, 49–51]. In the case of the Fe-Cu system it was pointed that Fe solution in Cu resulted in the increase of thermal stability but back process did not effect on grain growth [44].

The non-reactive magnetron sputtering of mixed TiN + TiB_2 targets allows to prepare the nanostructured one-phase nitride/boride films with both NaCl structure and AlB_2 one [4, 37, 50, 51]. Both the substoichiometric phases {Ti(N,B,C,O)$_{<1}$} and superstoichiometric ones {Ti(B,N,C,O)$_{>2}$} do not decompose after annealing up to 1000°C and retain their nanostructures after annealing (see further Table II) [51].

A theory of phase transformation in nanosized crystals developed in [53]. It was shown that the nucleation barrier and critical size of phase transformation are mainly dependent on the strain energy, interphase boundary energy and the grain size. The last effect can be ignored when grain size is more than 100 nm. These considerations were useful for the explanation of the different behaviour of martensitic transformation between nanocrystals of Fe-Ni and Ni-Ti alloys.

The interesting example of non-equilibrium phase changes is spinodal decomposition which observed in the systems of nanostructured alloys TiN-ZrN, TiC-ZrN, and TiN-AlN [4, 6, 22, 54]. Fig. 7 demonstrated the hardness increase for alloyed (Ti,Zr)N film after annealing at 1000°–1200°C a result of spinodal decomposition of TiN-ZrN solid solution which is accompanied by formation of a nanocrystalline structure verified by X-ray examination [22].

Such behaviour of the (Ti,Zr)N film at annealing gives us an interesting example of smart material which under high-temperature conditions can not only retain

TABLE II Average grain size (L, nm) and hardness (H_V, GPa) of as prepared and annealed nitride/boride films [51]

		As prepared		$T_{anneal} = 700$°C		$T_{anneal} = 1000$°C	
Film	Structure type	L	H_V	L	H_V	L	H_V
TiN	NaCl	9.9 ± 8.8	36–40	13.0 ± 6.6	38–42	10.2 ± 7.0	33–40
Ti(N,B)	NaCl	5.4 ± 4.0	53–59	8.1 ± 4.4	52–58	7.9 ± 3.8	32–42
Ti(B,N)	AlB_2	2.9 ± 1.1	46–52	3.7 ± 1.2	47–54	3.4 ± 1.9	38–45

hardness but also increase it partly. The annealing of nanocomposite (Ti,Al)N–Si_3N_4 at 800°C has revealed also the maximum hardness value and the minimum grain size which can be also attributed as a result of spinodal decomposition of (Ti,Al)N [55].

2.4. Relaxation and diffusion

2.4.1. Behaviour of residual stresses

A general analysis of relaxation processes in some nanocrystalline compounds is given in review [56]. It is known that relaxation of residual stresses comes before grain growth. The stress relaxation is accompanied by a decrease in XRD peak width because of the inhomogeneous strain reducing. In the case of NMs obtained by severe plastic deformation, high energy consolidation methods, and film/coating technology (see Table I) the relaxation processes are of particular importance.

Table II shows the annealing effect on grain size and hardness of nitride/boride films prepared by magnetron sputtering [51]. As it was pointed early, the annealing of such films did not result in decomposition of nonequilibrium Ti(N,B) and Ti(B,N) phases. From Table II it is obvious that the grain size change is not considerable but there is some decrease of hardness. The hardness evolution can be attributed to the residual compressive stresses relaxation.

The intrinsic residual compressive stresses in nanostructured nitride and other films can be very significant due to the differences in the thermal expansion and elastic properties between the film and the substrate [4, 6]. For example, in nitride films the value of residual compressive stresses can be of 10 GPa [6]. The stress relaxation involves migration, redistribution, and annihilation of different defects as well as a grain boundary sliding which as a whole have diffusion nature. The apparent activation energies (eV at^{-1}) of stress relaxation for some nitride films are the following [6]:

TiN		Ti(N,C)	CrN
250°–430°C	400°–900°C	450°–900°C	240°–670°C
1.23	2.1	2.1–3.1	2.1–3.1

The absolute values of these data are near to the value of energy activation of nitrogen self diffusion in nitrides (which is more likely to be grain boundary diffusion rather than volume diffusion). Discussion of relaxation processes and evolution of nanostructures in metals, alloys, and intermetallics prepared by severe plastic deformation can be found in [9].

2.4.2. Homogenisation processes

The diffusion processes in NMs have been discussed in details in [2, 6, 9]. The information about interdiffusion is very important for the analysis of the multilayer thermal stability. As applied to nitride multilayers, interdiffusion studies of single-crystal TiN/NbN superlatties ($\lambda = 4.4$–12.3 nm) give the following values of the apparent activation (Q_a) for metal interdiffusion in different temperature intervals [56, 57]

T°C	<830	830–875	900–930
Q_a(eV)	1.2 ± 0.1	2.6 ± 0.1	4.5 ± 0.1

It is clear that the temperature dependent change of Q_a values reflects the shift of an interdiffusion mechanism, i.e., from the defect-mediated and grain boundary diffusion to the volume one. From this interdiffusion information, the lifetime of 8-nm period nitride multilayer is considered to be equal as 1 hr at 900°C [58]. This estimation seems reasonable and agrees in the main with the hardness thermal stability.

However, notice that there are some contradictory data on the long-term thermal stability of multilayers. On the one hand, it has been observed that the high hardness values of TiN/NbN and TiN/ZrN multilayer films ($\lambda = 20$ nm) disappeared after a long storage at room temperature (about 1–1.5 year and may be more) [4]. On the other hand, the two years ambient exposition did not change the giant magnetoresistance effect in the Fe/Cr superlattices ($\lambda = 1.5$–2.5 nm) [59]. It is likely that some difference in the nitride subjects behaviour [4, 57, 58] is connected with preparation conditions, namely, with cathodic are plasma deposition on steel substrates ($T_{substr} = 300$°C) [4, 22] and magnetron sputtering on MgO (001) single-crystal substrate ($T_{substr} = 700$°C) [57, 58].

3. Radiation, deformation, and chemical stability

3.1. Radiation effect

The information on the radiation effects in NMs is not at all comprehensive but tends to widening (e.g. [60–63]). Nanocrystalline ZrO_2-bulks ($Lo \sim 70$ nm) showed no amorphization, defect agglomeration or grain growth after irradiation with 4 MeV Kr ions up to dose of 2×10^{17} ions/cm^2 [60]. A monoclynic-tetragonal phase transformation in ZrO_2 after irradiation with 5×10^{17} ions/cm^2 has been observed. A significant grain growth has been revealed in nanostructured Pd bulks ($L_o \sim 10$ nm) after irradiation. The irradiation-induced crystalline-amorphous transition in the ZrO_2 nanoparticles with size of 3 nm embedded in amorphous SiO_2 matrices was described in [63]. The full amorphization was fixed after irradiation with 1 MeV Xe ions at the dose of 0.8–0.9 dpa (the amorphization start was at the dose of 0.3 dpa). At the same time, the Au nanoparticles with size of 3 nm did not amorphize after the same irradiation.

It is stated that the dislocation density increases and the residual stresses becomes more compressive in the ion implanted TiN films prepared by CVD technique [62]. Some differences between C and B ion implantations have been also observed in the TiN prepared by ion-plating method [61]. In the former case the hardness was decreased with formation of the amorphous region with the lamella structure being perpendicular to the ion irradiation direction. In the latter case (B implantation) the hardness increased with formation of spherical amorphous region.

There are some information on radiation stability of nanocarbon materials (e.g. [64–66]). The bombardment of C_{60} films by 400 eV He ions results in the C_{60} molecules decomposition with formation of an amorphous structure having graphite-like near order [64]. The nanocrystalline diamond formation during Ar ion irradiation of graphite was fixed at the fluence of $\sim 10^{22}$ cm^{-2} [65].

3.2. Structure stability during deformation

This question seems to be important for the superplasticity problems because grain growth during deformation is known to be intensified. It has been observed in the experimental works (see, for example, review [67]) and confirmed by a theoretical analysis [68]. The model of deformation grain growth [68] agrees with experimental results as applied to the structural ceramics such as oxide materials based on ZrO_2, Al_2O_3 and so on.

The detail study of low-temperature superplasticity in nanocrystalline nickel, a nanocrystalline aluminium alloy (1420-Al), and nanocrystalline nickel aluminide (Ni_3Al) also revealed grain growth [69]. In the case of nanocrystalline nickel the increase of grain growth was the maximum. Even at low homologous temperatures grain growth during deformation resulted to annihilation of Ni nanostructure. The effects of particles (in 1420-Al) and a kinetic barrier for the preferred atomic pairing between the atoms in Ni_3Al are considered to be main factors of the grain growth inhibition during superplastic deformation.

The important conclusion of authors [69] is that their 'results appear to eliminate the hope of obtaining superplasticity in pure metals having a grain size of 100 nm or less.' The reason is that the superplasticity temperature decrease is offset by a reduction in the grain-growth temperature.

3.3. Chemical stability

From general considerations it would be expected that the nanostructure features must intensify the interfacial reactions. Unfortunately, with the exception of some oxidation studies, this problem seems to have been investigated only as episodically and in many cases the nanostructure characterisation was not so detail. The oxidation of NMs has been studied in several works (e.g. [6, 50, 70–72]). The oxidation mechanism for TiN, (Ti,Al)N, CrN, and NbN films has been established [6]. The additions of Y to nitride multilayers tend to increase the resistance against oxidation corrosion [70]. The presence of Y and YO_x at the grain boundaries is consdered to play a decisive role in reducing bulk diffusion rates for both cation and anion diffusion. The significant thermal stability and oxidation resistance have been revealed for $AlN + TiB_2$ and $AlN + SiC + TiB_2$ films after heating up to 1500°C [71]. The fractography analysis showed that the microstructure of oxidised films remained unaltered and very close to the nanocrystalline one, i.e., the structural entities size was about 100 nm.

The onset temperature for the nano-diamond graphitization under Ar heat treatment was found to be 670°C, while that for oxidation is 496° [72]. These temperatures are much lower than those for bulk diamond and the difference is likely connected with the nanoparticles size.

The solid phase interfacial reactions for TiB_x film/(100)Si system have been studied after vacuum annealing in the temperature range 300–1000°C [73]. No evidence of apparent structural change in this temperature interval was found for TiB_x samples with a ratio of B/Ti_2. For substoichiometric compounds ($B/Ti < 2$), the formation of a titanium silicide layer at the interface and the formation of a stoichiometric TiB_2 layer at the surface were observed.

4. Conclusions

Present review devoted mainly to stability of consolidated NMs (Table I). This problem is also very important as regarding to porous, semiconductor, catalytic, carbon, polymer, biological and supramolecular NMs but their study is only in its infancy and now is very limited (e.g. [74–77]).

As it is evident from foregoing the information on the analysed NM stability is not uniform. The largest body of data is related to grain growth, whereas very little data has been published on the radiation, deformation and chemical stability so the further detailed investigations seems very important. However, the grain growth features also need the further study. The most interesting question is whether the very small crystallites can be thermally stable. In this connection it should be noted that NMs with very small crystallites having the sizes about of 1–2 nm have been prepared by film technology (see Table I and Ref. [37, 50, 51, 78, 79]). Recall that value of lattice parameter for TiN is about of 0.424 nm, i.e., in the l-nm TiN crystallite averages about 8 (2^3) elementary cells. Such NMs can be named the cluster-consolidated materials as opposed to the cluster-assembled ones (e.g. [3, 80]). Their stability study is undoubtedly of special interest.

Notice also that the NM stability depends strongly on the technology regimes. Many routes such as high pressure sintering, rate controlled sintering, sinter-forge, doping and precipitation hardening, multilayer preparation and so on seem to be useful (e.g. [9–11, 81–84]). However, we can not now evaluate the processing role not to say on the intelligent prediction.

The development of the NM stability theory is closely connected to many poorly known theoretical questions such as an application of statistical thermodynamics and thermodynamics of irreversible processes to the NM problems, the energy properties of interfaces and triple junctions in nanocrystallites, and so on. It is seen from the foregoing that only first steps have been taken in the study and understanding of the NM stability nature. There is no doubt that the NM effectiveness for many applications depends significantly on further progress in the stability study.

Acknowledgements

This research is sponsored by NATO's Scientific Affairs Division in the framework of the Science for Peace Program (Project No 973529).

References

1. H. GLEITER, *Acta mater.* **45** (2000) 1.
2. R. A. ANDRIEVSKI and A. M. GLEZER, *Phys. Met. Metallogr.* **88**(1) (1999) 45 (Engl. Transl.).
3. A. S. EDELSTEIN and R. C. CAMMARATA (Eds.), "Nanomaterials: Synthesis, Properties and Applications" (Institute of Physics, Bristol, 1996/1998).
4. R. A. ANDRIEVSKI, *J. Mater. Sci.* **32** (1997) 4463.
5. T. R. MALOW and C. C. KOCH, *Acta Mater.* **45** (1997) 2177.

6. L. HULTMAN, *Vacuum* **57** (2000) 1.
7. C. SURYANARAYANA and C. C. KOCH, *Hyperfine Interactions* **130** (2000) 5.
8. G. GOTTSTEIN and L. S. SHVINDLERMAN, *Acta Mater.* **50** (2002) 703.
9. Y. R. KOLOBOV, R. Z. VALIEV, G. P. GRABOVETSKAYA, A. P. ZHILIAEV, E. F. DUDAREV, K. V. IVANOV, M. B. IVANOV, O. A. KASHIN and E. V. NADEIKIN, "Grain-Boundary DiffusiUon and Properties of Nanostructured Materials"(Nauka, Novosibirsk, 2001) (in Russian).
10. R. CAHN, Materials Today Nov/Dec (2001) 13.
11. R.A. ANDRIEVSKI, *Russ. Chem. Rev.* **70**(10) (2002) (Engl. Transl.).
12. S. GANAPATHI, D. M. OWEN and A. H. CHOKSHI, *Scripta Met. Mater.* **25** (1991) 2699.
13. K. ISONISHI and K. OKAZAKI, *J. Mater. Sci.* **28** (1993) 3829.
14. T. SPASSOV and U. KOSTER, *ibid.* **28** (1993) 2789.
15. K. W. LIU and F. MUCKLICH, *Acta Mater.* **49** (2001) 395.
16. A. KUMPMAN, B. GUNTHER and H.-D. KUNZE, *Mater. Sci. Eng.* A **168** (1993) 165.
17. V. U. GERTSMAN and R. BIRRINGER, *Scripta Met. Mater.* **30** (1994) 577.
18. R. J. PEREZ, H. G. JIANG, C. P. DOGAN and E. J. LAVERNIA, *Metall. Mater. Trans.* A **29** (1998) 2469.
19. Y. ZHU and M. TANG, *Mater. Sci. Eng.* A **201** (1995) Ll.
20. T. KIZUKA, H. ICHINOSE and Y. ISHIDA, *J. Mater. Sci.* **29** (1994) 3107.
21. S. VEPREK, *J. Vac. Sci. Technol.* A **17** (1999) 2401.
22. R. A. ANDRIEVSKI, I. A. ANISIMOVA and V. P. ANISIMOV, *Thin Solid Films* **205** (1991) 171.
23. R. A. ANDRIEVSKI, I. A. ANISIMOVA, V. P. ANISIMOV, V. P. MAKAROV and V. P. POPOVA, *ibid.* **261** (1995) 83.
24. D.-G. KIM, T.-Y. SEONG and Y.-J. BAIK, *Surf. Coating Technol.* **153** (2002) 79.
25. W. BUCHGRABER, R. K. ISMAGALIEV, Y. R. KOLOBOV and N. M. AMIRKHANOV, in "Investigations and Applications of Severe Plastic Deformation," edited by T. C. Lowe and R. Z. Valiev (Kluwer Academic Publishers, Dordrecht, 2000) p. 267.
26. A. MICHELS, C. E. KRILL, H. EHRHARDT, R. BIRRINGER and D. T. WU, *Acta Mater.* **47** (1999) 2143.
27. R. KIRCHHEIM, *ibid.* **50** (2002) 413.
28. J. WEISSMULLER, *Nanostruct. Mater.* **3** (1993) 261.
29. C. E. KRILL, R. KLEIN, S. JANES and R. BIRRINGER, *Mater. Sci. Forum* **179–181** (1995) 443.
30. C. CSERHATI, I. A. SZABO and D. L. BEKE, *J. Appl. Phys.* **83** (1998) 3021.
31. J. WEISSMULLER, W. KRAUS, T. HAUBOLD, R. BIRRINGER and H. GLEITER, *Nanostruct. Mater.* **1** (1992) 439.
32. B. FARBER, E. CADEL, A. MENAND, G. SCHMITZ and R. KIRCHHEIM, *Acta Mater.* **48** (2000) 789.
33. Y. ESTRIN, G. GOTTSTEIN, E. RABKIN and L. S. SHVINDLERMAN, *Scripta Mater.* **43** (2000) 141.
34. L. I. TRUSOV, V. I. NOVIKOV, Y. A. LOPUKNOV and V. N. LAPOVOK, in "Physical Chemistry of Ultrafine Systems," edited by I. V. Tanaev (Nauka, Moscow, 1987) p. 67 (in Russian).
35. M. UPMANYU, D. J. SROLOVITZ, L. S. SCHVINDLERMAN and G. GOTTSTEIN, *Interface Sci.* **6** (1998) 287.
36. V. G. GRIAZNOV, I. A. POLONSKY, A. E. ROMANOV and L. I. TRUSOV, *Phys. Rev.* B **44** (1991) 42.
37. R. A. ANDRIEVSKI, G. V. KALINNIKOV and D. V. SHTANSKIY, *Phys. Solid State* **42** (2000) 760 (Engl. Transl.).
38. K. AUST, U. ERB and G. PALUMBO, in "Processing and Properties of Nanocrystalline Materials", edited by C. Suryanarayana, J. Singh and F. H. Froes (Warrendale, TMS, 1996) p. 11.
39. S. PROTASOVA and V. SURSAEVA, *Interface Sci.* **44** (2001) 307.
40. M. UPMANYU, D. J. SROLOWITZ, L. S. SHVINDLERMAN and G. GOTTSTEIN, *Acta Mater.* **50** (2002) 1405.
41. S. OKUDA, M.KOBIYAMA, T. INAMI and S. TAKAMURA, *Scripta Mater.* **44** (2001) 2009.
42. K. LU, *Nanostruct. Mater.* **2** (1993) 643.
43. R. DANNENBERG, E. STACH and J. R. GROZA, *J. Mater. Res.* **16** (2001) 1090.
44. J. ECKERT, J. C. HOLZER and W. L. JOHNSON, *J. Appl. Phys.* **73** (1993) 131.
45. T. ABOUD, B.-Z. WEISS and R. CHAIM, *Nanostruct. Mater.* **6** (1995) 405.
46. I. BAKER and F. LIU, *ibid.* **7** (1996) 13.
47. J. Y. HUANG, Y. D. YU, Y. K. WU, H. Q. YE and Z. F. DONG, *J. Mater. Res.* **11** (1996) 2717.
48. B.-L. HUANG, R. J. PEREZ, E. J. LAVARNIA and M. J. LUTON, *Nanostruct. Mater.* **7** (1996) 67.
49. V. V. TCHERDYNTSEV, S. D. KALOSHKIN, I. A. TOMILIN, E. V. SHELEKHOV and Y. V. BALDOKHIN, *ibid.* **12** (1999)139.
50. R. A. ANDRIEVSKI and G. V. KALINNIKOV, *Surf. Coating Technol.* **142–144** (2001) 573.
51. R. A. ANDRIEVSKI, G. V. KALINNIKOV, A. E. OBLEZOV and D. V. SHTANSKIY, *Doklady Acad. Sci.* **384** (2002) 36 (in Russian).
52. S. A. DREGIA, R. BANERJEE and H. L. FRAZER, *Scripta Mater.* **39** (1998) 217.
53. Q. MENG, Y. RONG and T. Y. HSU, *Phys. Rev.* **65B** (2002) 174118.
54. O. KNOTEK and A. BARIMANI, *Thin Solid State* **174** (1989) 51.
55. H.-D. MANNLING, D. S. PATIL, K. MOTO, M. JILEK and S. VEPREK, *Surf. Coating Technol.* **146/147** (2001) 263.
56. L. N. LARIKOV, *Metaphysics and Advanced Technology* **19** (1997) 20 (in Russian).
57. C. ENGSTROM, J. BIRCH, L. HULTMAN, C. LAVOIE, C. CABRAL, J. L. JORDAN-SWEET and J. R. A. CARLSSON, *J. Vac. Sci. Technol.* A **17** (1999) 2920.
58. L. HULTMAN, C. ENGSTROM and M. ODEN, *Surf. Coating Technol.* **133/134** (2000) 227.
59. L. N. ROMASHEV, A. B. RYNKEVICH, V. V. USTINOV, A. A. YUVCHENKO and A. M. BURKHANOV, *Defectoscopy* **7** (2001) 3 (in Russian).
60. R. ROSE, G. GORZAWSKI, G. MIEHE, A. G. BALOGH and H. HAHN, *Nanostruct. Mater.* **6** (1995) 731.
61. H. OHARA, A. NAKAYAMA and T. NOMURA, *J. Vac. Sci. Technol*, A **15** (1997) 2609.
62. A. J. PERRY, *Mater. Sci. Eng.* A **253** (1998) 310.
63. A. MELDRUM, L. A. BOATNER and R. C. EWING, *Phys Rev. Lett.* **88** (2002) 025503.
64. A. V. VASIN, L. A. MATVEEVA, V. A. JUKHIMCHUK and E. M. SHPILEVSKI, *Letters in JTF* **27** (2001) 65 (in Russian).
65. Z. WANG, G. YU, L. YU, F. ZHU, D. ZHU and H. XU, *J. Appl. Phys.* **91** (2002) 3480.
66. A. V. KRASHENINNIKOV, K. NORDLUND and J. KEINONEN, *Phys. Rev.* B **65** (2002) 165423.
67. R. A. ANDRIEVSKI and A. M. GLEZER, *Phys. Met. Metallogr.* **89**(1) (2000) 83 (English Transl.).
68. V. N. PEREVEZENTSEV, O. E. PIROZHNIKOVA and V. N. CHUVIL'DIEV, *Inorg. Mater.* **29** (1993) 421 (in Russian).
69. S. X. MCFADDEN, R. S. MISHRA, R. Z. VALIEV, A. P. ZHILYAEV and A. K. MUKHERJEE, *Nature* **398** (1999) 684.
70. W.-D. MUNZ, D. B. LEWIS, P. E. HOVSEPIAN, C. SCHONJAHN, A. EHIASARIAN and I. J. SMITH, *Surface Eng.* **17** (2001) 15.
71. R. A. ANDRIEVSKI, V. A. LAVRENKO, J. DESMAISON, M. DESMAISON-BRUT, G. V. KALINNIKOV and A. D. PANASYUK, *Doklady Physical Chemistry* **373** (2000) 99.
72. N. S. XU, J. CHEN and S. Z. DENG, *Diamond and Related Materials* **11** (2002) 249.
73. Y.-K. LEE, J.-Y. KIM, Y.-K. LEE, G.-S. EOM, Y.-K. KWON, M.-S. LEE, C.-M. LIN, D.-K. KIM, Y.-C. JIN and D.-K. PARK, *J. Mater. Sci.* **37** (2002) 515.
74. M. W. ANDERSON, J. R. AGGER, N. HANIF and O. TERASAKI, *Microporous and Mesoporous Materials* **48** (2001) 1.

75. W. ZHANG, X. HAN, X. LIU and X. BAO, *ibid.* **50** (2001) 13.
76. N. Y. JIN-PHILLIPP, K. DU, F. PHILLIPP, M. ZUNDEL and K. EBERL, *J. Appl. Phys.* **91** (2002) 3255.
77. S. T. PURCELL, P. VINCENT, C. JOURNET and V. T. BINH, *Phys. Rev. Lett.* **88** (2002) 105502.
78. A. A. VOEVODIN, J. P. O'NEIL and J. S. ZABINSKI, *Surf. Coating Technol.* **116–119** (1999) 36.
79. D. V. SHTANSKI, K. KANEKO, Y. IKUHARA and E. A. LEVASHOV, *ibid.* **148** (2001) 204.
80. R. SIEGEL, in "Materials Science and Technology. Processing of Metals and Alloys," Vol. 15, edited by R. Cahn (VCH, Weinheim, 1991) p. 583.
81. R. A. ANDRIEVSKI, in "Functional Gradient Materials and Surface Layers Prepared by Fine Particles," edited by M.-I. Baraton and I. Uvarova (Kluwer Academic Publishers, Dordrecht, 2001) p. 17.
82. A. V. RAGULYA, Doctor Science Thesis, Institute for Problems in Materials Science, Kiev. Ukraine, 2001 (in Russian).
83. J. MARKAMANN, A. TSCHOPE and R. BIRRINGER, *Acta Mater.* **50** (2002) 1433.
84. A. VINOGRADOV, V. PATLAN, Y. SUZUKI, K. KITAGAWA and V. I. KOPYLOV, *ibid.* **50** (2002) 1639.

Received 25 October
and accepted 16 December 2002